Monte Carlo ICRH simulations in fully shaped anisotropic plasmas

M. Jucker, J.P. Graves, W.A. Cooper, N. Mellet and S. Brunner

Ecole Polytechnique Fédérale de Lausanne (EPFL), Centre de Recherches en Physique des Plasmas, CH-1015 Lausanne, Switzerland

Abstract. In order to numerically study the effects of Ion Cyclotron Resonant Heating (ICRH) on the fast particle distribution function in general plasma geometries, three codes have been coupled: VMEC[1] generates a general (2D or 3D) MHD equilibrium including full shaping and pressure anisotropy. This equilibrium is then mapped into Boozer coordinates. The full-wave code LEMan[2], [3] then calculates the power deposition and electromagnetic field strength of a wave field generated by a chosen antenna using a warm model. Finally, the single particle Hamiltonian code VENUS[4, 5] combines the outputs of the two previous codes in order to calculate the evolution of the distribution function. Within VENUS, Monte Carlo operators for Coulomb collisions of the fast particles with the background plasma have been implemented, accounting for pitch angle and energy scattering. Also, ICRH is simulated using Monte Carlo operators on the Doppler shifted resonant layer. The latter operators act in velocity space and induce a change of perpendicular and parallel velocity depending on the electric field strength and the corresponding wave vector. Eventually, the change in the distribution function will then be fed into VMEC for generating a new equilibrium and thus a self-consistent solution can be found. This model is an enhancement of previous studies in that it is able to include full 3D effects such as magnetic ripple, treat the effects of non-zero orbit width consistently and include the generation and effects of pressure anisotropy. Here, first results of coupling the three codes will be shown in 2D tokamak geometries.

Keywords: Monte Carlo simulations, RF heating, Pressure anisotropy
PACS: 52.50.Qt, 52.55.Fa, 52.65.Cc, 52.65.Pp, 52.65.Rr

INTRODUCTION

In present day fusion devices, radio frequency (RF) heating of minority species becomes more and more important. Especially, RF heating in the ion cyclotron range of frequencies (ICRH) is considered to be one of the major contributors to additional heating in ITER and other machines. Moreover, 3D effects such as magnetic ripple are expected to be important not only in stellarators, but also in ITER. This work proposes a 3D self-consistent numerical approach for studying the effects of ICRH on the equilibrium quantities such as temperature, density and pressure. First, the MHD equilibrium and stability codes VMEC[1] and TERPSICHORE [6, 7] (the latter used for mapping into Boozer coordinates) have been updated for including the effects of an anisotropic distribution function which can be written as [8]

$$F_h(\psi,E,\mu) = \left(\frac{m}{2\pi}\right)^{3/2} \frac{n_c(\psi)}{T_\perp(\psi)T_\parallel^{1/2}(\psi)} \exp\left[-\frac{\mu B_c}{T_\perp(\psi)} - \frac{|E-\mu B_c|}{T_\parallel(\psi)}\right], \qquad (1)$$

where m is the mass of the particle, n_c the hot particle density at $B = B_c$, $E = mv^2/2$ the particle energy, $\mu = mv_\perp^2/2B$ the magnetic moment, $T_{\perp,\parallel}$ the perpendicular/parallel temperature and ψ a flux label. Also, the VENUS code has been updated to incorporate the effects of anisotropic pressure within the Hamiltonian equations of motion [9].

Recently, a new module has been added to the VENUS code which calculates the new pressure and temperature profiles including the effects of Coulomb collisions of the fast ions on the background plasma and an ICRF wave field. This wave field is calculated using the full-wave code LEMan, which has also been updated in order to include anisotropic equilibria. The derivation of the corresponding dielectric tensor is shown in the next section.

DIELECTRIC TENSOR

Following Refs. [10, 11], we have derived the dielectric tensor for the fast particles modelled by the distribution function (1) to zeroth order in both $\varepsilon_e = \rho/L$ and $\varepsilon_p = \rho/\lambda_\perp$, where ρ is the Larmor radius, L a characteristic length scale of the stationary plasma and $\lambda_\perp$ a characteristic wave length of the perturbing electromagnetic field in the poloidal direction. We linearise the Vlasov equation, introduce the cylindrical variables in velocity space $(v_\perp, \alpha, v_\parallel)$ and pass into Fourier space for the variables (t, y, z, α). We then find equations for the perturbed Fourier amplitudes f_n as a function of the velocity derivatives of the equilibrium distribution function, where n is the mode number with respect to the pitch angle α. The perturbed current density becomes finally [11]

$$\mathbf{j} = \sum_s q\pi \int_0^\infty v_\perp dv_\perp \int_{-\infty}^\infty dv_\parallel \left\{ v_\perp \left[(f_1 + f_{-1})\hat{\mathbf{x}} + i(f_1 - f_{-1})\hat{\mathbf{y}} \right] + 2v_\parallel f_0 \hat{\mathbf{z}} \right\}, \qquad (2)$$

where the sum is over all species. For the calculation of $f_{\pm 1}$ and f_0 we use the equilibrium distribution function given by Eq. (1). Finally, the dielectric tensor can be found with $\mathbf{j} = \sigma\mathbf{E}$ and $\mathscr{E} = \mathbf{1} - i\sigma/\omega\varepsilon_0$. The calculations are somewhat lengthy and therefore not presented here. The resulting dielectric tensor is

- For $B \geq B_c$:

$$\mathscr{E}_{xx} = \mathscr{E}_{yy} = 1 - \frac{1}{2\omega} \sum_s A^+ (\tilde{Z}_1 + \tilde{Z}_{-1}) \qquad (3a)$$

$$\mathscr{E}_{xy} = -\mathscr{E}_{yx} = -\frac{i}{2\omega} \sum_s A^+ (\tilde{Z}_1 - \tilde{Z}_{-1}) \qquad (3b)$$

$$\mathscr{E}_{\parallel\parallel} = 1 + 2 \sum_s \frac{A^+}{(k_\parallel v_{\parallel T})^2} \left(\omega_p^2 - \omega \tilde{Z}_0 \right), \qquad (3c)$$

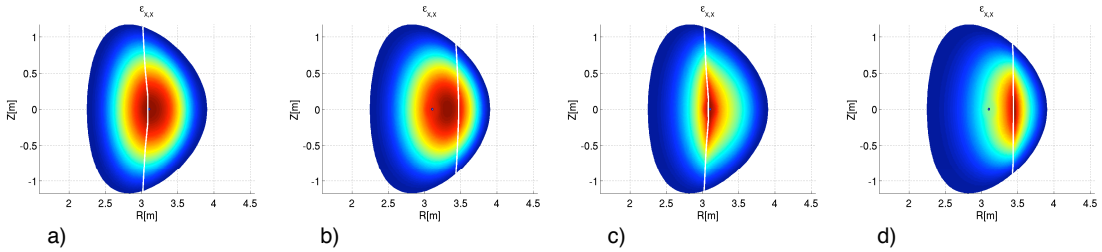

FIGURE 1. Value of first element of the hot particle dielectric tensor. The white line indicates where $B = B_c$: a) & b) On-axis heating, b) & d) off-axis heating. a) & b) isotropic, c) & d) anisotropic ($T_\perp/T_\parallel$=10) case.

- For $B < B_c$:

$$\mathscr{E}_{xx} = \mathscr{E}_{yy} = \mathscr{E}_{xx}^{B\geq B_c} + \frac{1}{2\omega}\sum_s A^+ \sqrt{\frac{A^-}{2}\frac{B}{B_c}}\left(\frac{A^- - A^+}{A^+}\right)^{3/2}(\tilde{Z}_1^c + \tilde{Z}_{-1}^c) \quad (4a)$$

$$\mathscr{E}_{xy} = -\mathscr{E}_{yx} = \mathscr{E}_{xy}^{B\geq B_c} + \frac{i}{2\omega}\sum_s A^+ \sqrt{\frac{A^-}{2}\frac{B}{B_c}}\left(\frac{A^- - A^+}{A^+}\right)^{3/2}(\tilde{Z}_1^c - \tilde{Z}_{-1}^c) \quad (4b)$$

$$\mathscr{E}_{\parallel\parallel} = \mathscr{E}_{\parallel\parallel}^{B\geq B_c} - 2A^- \sqrt{\frac{T_\perp}{T_\parallel}}\frac{B_c}{B}\sqrt{1-\frac{B}{B_c}}(\omega_p^2 - \omega\tilde{Z}_0^c), \quad (4c)$$

Here, $v_{\parallel T}^2 = T_\parallel/2m$ is the fast particles' thermal parallel velocity and

$$A^\pm = \frac{B_c}{B} \pm \frac{T_\perp}{T_\parallel}\left(1-\frac{B_c}{B}\right), \qquad Z^{Sh}(z) = \frac{z}{\sqrt{\pi}}\int_{-\infty}^{\infty}\frac{1}{z-x}e^{-x^2}dx, \qquad \mathrm{Im}z > 0, \quad (5)$$

$$\tilde{Z}_l = \frac{\omega_p^2}{\omega - l\Omega_c}Z^{Sh}\left(\frac{\omega - l\Omega_c}{k_\parallel v_{\parallel T}}\right) \quad \text{and} \quad \tilde{Z}_l^c = \frac{\omega_p^2}{\omega - l\Omega_c}Z^{Sh}\left(\frac{\omega - l\Omega_c}{k_\parallel v_{\parallel T}}\sqrt{\frac{B_c}{B_c - B}}\right) \quad (6)$$

and ω_p^2 the plasma frequency of the species s. We can highlight a few observations: First of all, one can see that we exactly recover the zeroth order results obtained in Refs. [11] and [10] in the limit where $T_\perp/T_\parallel \to 1$ and $B_c \to 0$ (i.e. $F_h \to F_M$). However, the additional parameter B_c in the distribution function has the effect that even if we consider the isotropic case $T_\perp = T_\parallel$, some of the additional terms do not vanish and introduce poloidally dependent corrections to the dielectric tensor.

NUMERICAL RESULTS

Dielectric tensor

A more intuitive understanding of what happens to the dielectric tensor can be obtained when we compare the two cases graphically. Fig. 1 shows the dielectric tensor

element $\mathscr{E}_{xx}$ in both the isotropic and the anisotropic case for on- and off-axis heating. The equilibria used for the calculations are JET-like (R_0=3.1, a=1m, κ_a=1.4, δ=0.4, B_0=3.38T) and done keeping beta constant with values of $\beta_{tot} = 0.5\%$ and $\beta_h = 0.2\%$ for total and hot beta respectively. We chose a background composed of thermal deuterium ions and electrons and minority heating on hydrogen fast ions at the first harmonic, which is at 52/46 MHz for on-/off-axis heating respectively, which corresponds to B_c=3.38/3.00T. For the chosen densities (thermal particles n_{th}=$2\times10^{19}(1-s)$, hot particle density $n_h = 0.05 n_{th}(1-s)$), the ICRF power deposition was one order of magnitude higher on the fast ions than on the background plasma.

In Fig. 1 one can easily see the poloidal dependence of the dielectric tensor in the anisotropic cases c) and d). Also, the region of high values of the dielectric tensor are clearly much more localised around the resonant layer in the isotropic case.

Temporal evolution

In order to study the effects of ICRH on the fast particles, the schematics shown hereafter have been implemented. The different stages are as follows:

(1) The equilibrium is calculated using the anisotropic version of VMEC[7] and converted into Boozer coordinates by TERPSICHORE.

(2) In order to calculate the wave field and power deposition, LEMan is used with a warm model and incorporating the newly derived anisotropic dielectric tensor. Minority heating on hydrogen ions in a background of deuterium ions and electrons is used.

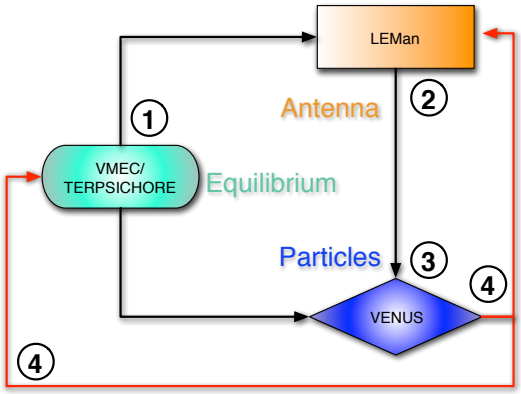

(3) The evolution of the distribution function is simulated with the single particle Hamiltonian code VENUS, including Monte Carlo operators for Coulomb scattering and ICRF heating.

(4) The updated distribution function moments are fed back into VMEC and LEMan for the next cycle.

The implemented Monte Carlo operators are equal to those described in Ref. [12] and include pitch angle and energy scattering due to Coulomb collisions on the background ions and electrons as well as kicks in perpendicular and parallel velocity due to the ICRF wave field. Note that we do not include explicit kicks in the toroidal canonical momentum P_ϕ, since the corresponding effects (such as radial diffusion of trapped particles [13]) are intrinsically included in the following of the particle's orbits. The kicks in velocity space are proportional to the magnitude of the electric field and are only applied when a particle crosses the Doppler shifted resonant layer, i.e. when $\omega_{rf} - k_{\|} v_{\|} = n\Omega_c$, where ω_{rf} is the wave frequency, Ω_c the cyclotron frequency of the

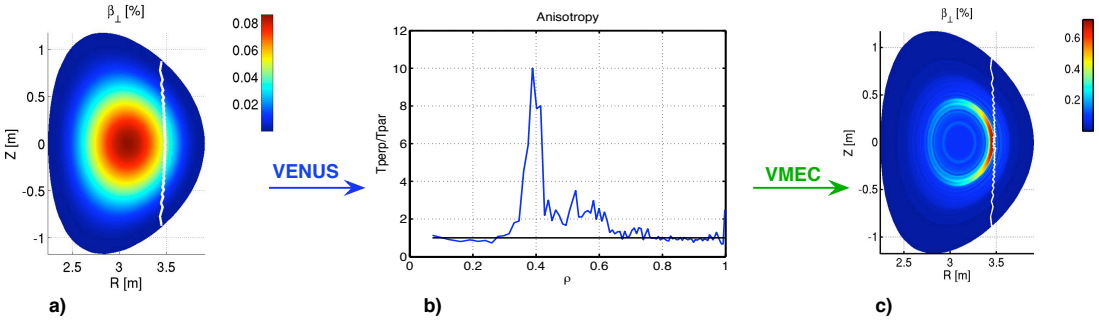

FIGURE 2. Effect of ICRH on the perpendicular pressure through anisotropy after one iteration. $\beta_\perp = 2\mu_0 p_\perp / B_0^2$. a) Initial $\beta_\perp$ surfaces, b) newly developed anisotropy after one run, d) $\beta_\perp$ surfaces after first iteration. The white line represents the resonant layer $B = B_c$.

fast ions and n the label of the harmonic.

After each VENUS run, new inputs to LEMan and VMEC have to be computed. For this, first the moments of the hot distribution function $n_h(\psi,\theta), p^h_{\parallel,\perp}(\psi,\theta)$ are computed as described in Ref. [8] and then the relations presented in Ref. [7] for $B \geq B_c$ are used. The needed inputs are the anisotropy $T_\perp/T_\parallel$ and the hot pressure amplitude p_h for VMEC and additionally the hot particle density and parallel temperature for LEMan. In order to find these, we move from the centre along $\theta = 0$ (using $B \geq B_c$) until we hit the resonant layer and then follow the latter to the wall (using $B = B_c$). The explicit relations are [7]

$$\frac{T_\perp}{T_\parallel}(\psi) = \frac{\frac{B_c}{B}\frac{p_\perp(\psi,\theta)}{p_\parallel(\psi,\theta)}}{1+\frac{B_c}{B}\frac{p_\perp(\psi,\theta)}{p_\parallel(\psi,\theta)}\left(1-\frac{B}{B_c}\right)}, \qquad T_\parallel(\psi) = \frac{p^h_\parallel(\psi,\theta)}{n_h(\psi,\theta)}\sqrt{\frac{T_\parallel}{T_\perp}}, \tag{7a}$$

$$p_h(\psi) = \frac{p^h_\parallel(\psi,\theta)}{p_{th}(\psi)H(\psi,B)}, \qquad H(\psi,\theta) = \frac{B/B_c}{1-T_\perp/T_\parallel\,(1-B/B_c)}. \tag{7b}$$

Figure 2 shows one complete iteration of the code as described above. We start with an isotropic equilibrium, where the thermal beta is about ten times higher than the hot particle beta. The initial parameters are $R_0 = 3.1$m, $a = 0.95$m, $\kappa_a = 1.4$, $\delta_a = 0.4$, $B_0 = 3.4$T, $B_c = 3$T, $\beta_{th} = 0.3\%$, $\beta_h = 0.02\%$, $T_{th} = 5$keV, $T_{\perp,h} = 65$keV. The wave frequency is $f = 46$MHz, the total absorbed power is 7MW and the simulation is stopped arbitrarily after 10ms.

As expected, we see that even if we start from an isotropic equilibrium, ICRH has its effect not only in raising the hot particle's temperature, but more precisely mainly raising the hot particle's perpendicular temperature and thus creating an anisotropic equilibrium. Fig. 2b) shows that perpendicular anisotropy develops at the resonant layer around $\rho \approx 0.4$. It is worth noting that this first iteration represents the first time a non-constant (in radius) anisotropy was fed into VMEC.

It is important to note here that Fig. 2 is not to be understood as real physical result: We have stopped the simulation arbitrarily after 10ms without any requirement of convergence to a physical state. Here, the emphasis is on the feasibility of such a numerical model rather than the physical results themselves. The next step is to iterate

the cycle more often until a certain saturation is reached where the equilibrium does not change anymore. This would then represent an equilibrium we would expect for long time ICRF heating at the chosen frequency in the considered plasma. This work is still in progress and no such results can therefore be shown here.

CONCLUSIONS

We have presented here a self-consistent numerical model for simulating the effects of ion cyclotron heating in an arbitrary (2D or 3D), fully shaped plasma. The dielectric tensor for an anisotropic plasma has been derived and implemented into the full-wave code LEMan. It could then be shown that the anisotropic dielectric tensor becomes dependent on poloidal angle. Then, the codes VMEC and TERPSICHORE for the equilibrium, LEMan for the wave field and VENUS for the evolution of the distribution function have been coupled and a first iteration could be demonstrated. As expected, we see a developing of perpendicular anisotropy at the resonant layer and as a result a poloidally localised raising of the perpendicular pressure.

In the near future, several iterations will be necessary in order to find a converged equilibrium where Coulomb collisions and ICRH balance each other. Also, numerical convergence studies and benchmarks with other codes will have to be performed. It will also be interesting to explore the changing of the dielectric tensor due to growing anisotropy and its effect on the wave field and ultimately the particle orbits.

ACKNOWLEDGMENTS

This work was supported in part by the Swiss National Science Foundation. Also, the authors would like to acknowledge the help of L. Villard.

REFERENCES

1. W. Cooper, S. Hirshman, S. Merazzi, and R. Gruber, *Comp. Phys. Comm.* **72**, 1 (1992).
2. P. Popovich, W. Cooper, and L. Villard, *Comp. Phys. Comm.* **175**, 250 (2006).
3. N. Mellet, P. Popovich, W. Cooper, L. Villard, and S. Brunner, *Theory of Fusion Plasmas: Varenna-Lausanne International Workshop* p. 382 (2006).
4. O. Fischer, W. Cooper, M. Isaev, and L. Villard, *Nucl. Fusion* **42**, 817 (2002).
5. M. Jucker, J. Graves, G. Cooper, and W. Cooper, *Plasma Phys. Control. Fusion* **50**, 065009 (2008).
6. D. Anderson, W. Cooper, G. Fu, M. Gengler, R. Gruber, S. Merazzi, and U. Schwenn, *Supercomp. Rev.* **3**, 29 (1991).
7. W. Cooper, J. Graves, S. Hirshman, T. Yamaguchi, Y. Narushima, S. Okamura, S. Sakakibara, C. Suzuki, K. Watanabe, H. Yamada, and K. Yamazaki, *Nucl. Fusion* **46**, 683 (2006).
8. J. P. Graves, K. I. Hopcraft, R. O. Dendy, R. J. Hastie, K. G. McClements, and M. Mantsinen, *Phys. Rev. Lett.* **84**, 1204–1207 (2000).
9. G. Cooper, M. Jucker, W. Cooper, J. Graves, and M. Isaev, *Phys. Plasmas* **14**, 102506 (2007).
10. S. Brunner, and J. Vaclavik, *Phys. Fluids B* **5**, 1695 (1993).
11. T. Martin, and J. Vaclavik, *Helvetica Physica Acta* **60**, 471–479 (1987).
12. M. A. Kovanen, and W. G. F. Core, *J. Comp. Phys* **105**, 14 (1993).
13. J. Hedin, T. Hellsten, and L.-G. Eriksson, *Nucl. Fusion* **40**, 1819 (2000).